Balance between cell–substrate adhesion and myosin contraction determines the frequency of motility initiation in fish keratocytes

Erin Barnhart[a,1], Kun-Chun Lee[b,1], Greg M. Allen[a], Julie A. Theriot[a,c,2,3], and Alex Mogilner[d,e,2,3]

[a]Department of Biochemistry and Howard Hughes Medical Institute, Stanford University School of Medicine, Stanford, CA 94305; [b]Department of Neurobiology, Physiology and Behavior, University of California, Davis, CA 95616; [c]Department of Microbiology and Immunology, Stanford University, Stanford, CA 94305; and [d]Courant Institute of Mathematical Sciences and [e]Department of Biology, New York University, New York, NY 10012

Edited by Herbert Levine, Rice University, Houston, TX, and approved March 11, 2015 (received for review September 9, 2014)

Cells are dynamic systems capable of spontaneously switching among stable states. One striking example of this is spontaneous symmetry breaking and motility initiation in fish epithelial keratocytes. Although the biochemical and mechanical mechanisms that control steady-state migration in these cells have been well characterized, the mechanisms underlying symmetry breaking are less well understood. In this work, we have combined experimental manipulations of cell–substrate adhesion strength and myosin activity, traction force measurements, and mathematical modeling to develop a comprehensive mechanical model for symmetry breaking and motility initiation in fish epithelial keratocytes. Our results suggest that stochastic fluctuations in adhesion strength and myosin localization drive actin network flow rates in the prospective cell rear above a critical threshold. Above this threshold, high actin flow rates induce a nonlinear switch in adhesion strength, locally switching adhesions from gripping to slipping and further accelerating actin flow in the prospective cell rear, resulting in rear retraction and motility initiation. We further show, both experimentally and with model simulations, that the global levels of adhesion strength and myosin activity control the stability of the stationary state: The frequency of symmetry breaking decreases with increasing adhesion strength and increases with increasing myosin contraction. Thus, the relative strengths of two opposing mechanical forces—contractility and cell–substrate adhesion—determine the likelihood of spontaneous symmetry breaking and motility initiation.

symmetry breaking | cell migration | adhesion | myosin

Stationary adherent cells are symmetric systems, in which all forces generated by and acting on the cell are balanced, allowing the cell to maintain a consistent shape and position. In order for a stationary cell to initiate motility, the symmetry of the system must first be broken by external or internal cues. Mechanisms of symmetry breaking have been extensively studied in chemotactic cells, such as neutrophils and *Dictyostelium*, which break symmetry and migrate in the direction of chemoattractant gradients (1). However, stationary neutrophils also break symmetry and initiate motility in uniform baths of chemoattractant (2, 3), indicating that a directional cue is not required. In addition, nonchemotactic cells, including fish epithelial keratocytes and keratocyte fragments, are able to break symmetry and initiate motility in the absence of external cues (4, 5). Thus, while external cues may confer a preferred directionality, intrinsic cellular instabilities can be sufficient for symmetry breaking.

Spontaneous symmetry breaking requires nonlinear amplification of stochastic fluctuations in chemical or mechanical signals (6). To understand how cellular systems break symmetry, it is necessary to answer three questions. First, what are the relevant fluctuations that drive symmetry breaking? Second, how are those fluctuations amplified in time and space? Finally, what sets the instability threshold—i.e., what determines the magnitude of the initial fluctuations that are required before the system breaks symmetry? Feedback between diffusible chemical activators and inhibitors can trigger biochemical instabilities (often called "Turing instabilities") that result in symmetry breaking (7); notable cellular examples include Min protein oscillations in *Escherichia coli* (8) and polarization and symmetry breaking in budding yeast (9). Mechanical instabilities can also drive symmetry breaking and have been shown to be particularly relevant for force-generating cytoskeletal systems (10–12). Stochastic fluctuations in actin filament densities and mechanical feedback between motor proteins and cytoskeletal elements can drive symmetry breaking, as in reconstituted actin-based rocketing motility of bacterial pathogens (13–15) and during asymmetric division of the *Caenorhabditis elegans* embryo (16, 17). Synthetic biology experiments have shown that both positive feedback and mutual inhibition are sufficient for symmetry breaking under limited conditions; combining multiple feedback loops promotes symmetry breaking under broader sets of conditions (18).

Feedback among multiple mechanical systems is likely to contribute to symmetry breaking and initiation of cell migration (5). Symmetry breaking is associated with rearrangement of actin polymerization and actin network flow patterns (5), and stochastic fluctuations in the mechanical systems that govern either actin polymerization or flow could, in principle, trigger symmetry breaking. Previous work has shown that increased myosin activity

Significance

Symmetry breaking and motility initiation are required for many physiological and pathological processes, but the mechanical mechanisms that drive symmetry breaking are not well understood. Fish keratocytes break symmetry spontaneously, in the absence of external cues, with myosin-driven actin flow preceding rear retraction. Here we combine experimental manipulations and mathematical modeling to show that the critical event for symmetry breaking is a flow-dependent, nonlinear switch in adhesion strength. Moreover, our results suggest that mechanical feedback among actin network flow, myosin, and adhesion is sufficient to amplify stochastic fluctuations in actin flow and trigger symmetry breaking. Our mechanical model for symmetry breaking in the relatively simple keratocyte provides a framework for understanding motility initiation in more complex cell types.

Author contributions: E.B., J.A.T., and A.M. designed the experiments; E.B. and G.M.A. performed the experiments; E.B. analyzed the data; K.-C.L. and A.M. wrote the mathematical model and carried out model simulations; and E.B., J.A.T., and A.M. wrote the paper.

The authors declare no conflict of interest.

This article is a PNAS Direct Submission.

[1]E.B. and K.-C.L. contributed equally to this work.

[2]J.A.T. and A.M. contributed equally to this work.

[3]To whom correspondence may be addressed. Email: mogilner@cims.nyu.edu or theriot@stanford.edu.

This article contains supporting information online at www.pnas.org/lookup/suppl/doi:10.1073/pnas.1417257112/-/DCSupplemental.

in the prospective cell rear of stationary fish keratocytes results in increased centripetal flow of the actin network, rear retraction, and motility initiation (5), and myosin contraction has been shown to contribute to symmetry breaking by defining the cell rear in other cell types as well (19, 20). Moreover, myosin II minifilaments bind and move with the actin network, resulting in positive feedback between myosin localization and actin network flow: Myosin activity drives actin flow, resulting in the accumulation of more actin-bound myosin. This positive feedback between myosin and actin flow is thought to be required for symmetry breaking in fish keratocytes (5).

The forces generated by myosin-dependent actin flow are transmitted to the substrate by adhesion complexes, but the manner in which adhesions contribute to symmetry breaking is not well understood. Cell–substrate adhesions are dynamic structures, composed of molecules that link the actin network to adhesion receptors on the cell surface, which, in turn, bind to ligands on the substrate (21). The dynamic coupling of the actin network with the underlying substrate, via populations of adhesion molecules, generates a frictional slippage interface between the cell and the surface (22). Forces generated by myosin-dependent actin flow are transmitted to the substrate via this frictional interface, resulting in traction force generation. We have previously found that alterations in cell–substrate adhesion change the magnitude of myosin-driven actin network flow in motile keratocytes (23), raising the question of how variations in cell–substrate adhesion might contribute to changes in the spatial pattern of actin network flow during the process of symmetry breaking and motility initiation for stationary cells.

In this work, we have combined traction force measurements with experimental manipulations of cell–substrate adhesion and myosin activity and mathematical modeling to understand the contribution of adhesion- and myosin-dependent feedback loops to symmetry breaking and motility initiation in fish keratocytes. Our model simulations and experimental evidence suggest that stochastic fluctuations in adhesion strength and myosin activity trigger an actin flow-dependent, nonlinear switch in adhesion strength that results in symmetry breaking and persistent motility.

Results

Stationary Cells Have Stronger Adhesions Than Motile Cells. Stationary, radially symmetric keratocytes exhibit slow centripetal actin network flow (5). Slow actin network flow can be associated with either weak traction force generation or strong traction force generation, depending on the state of the adhesions (24). To determine whether stationary keratocytes are in a low-traction or high-traction regime, we first set out to characterize the spatial organization of the adhesion–contraction force balance system in stationary and motile keratocytes under comparable conditions. To do this, we directly measured traction force and actin flow patterns for cells in both configurations, as well as the distribution of myosin II and adhesion-related proteins (Fig. 1). To measure traction forces in stationary and motile cells, we plated keratocytes on polyacrylamide (PAA) gels with fluorescent beads embedded in the top layer of the gel and measured traction stress fields from cell-induced bead displacements (25). We found that motile keratocytes primarily exert traction forces perpendicular to the direction of cell movement, with slight rearward traction forces at the cell front (Fig. 1*A*), consistent with previous work (26, 27). Stationary cells, in contrast, display centripetal traction force patterns (Fig. 1*A*). Stationary cells generate substantially higher traction forces (average traction force = 46.2 Pa, $n = 10$ cells) compared with motile cells (28.8 Pa at the leading edge, and 7.7 Pa in the rear, $n = 9$ cells; Fig. 1*F*). Adhesions in stationary cells are also larger and more elongated than adhesions in motile cells (Fig. 1*C*).

Next, we used quantitative actin speckle microscopy (5, 28) to measure actin network flow (Fig. 1 *B* and *G*). We found, as

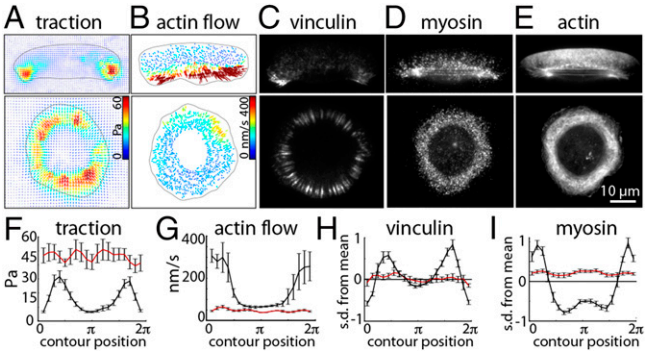

Fig. 1. Traction force, actin flow, adhesion, and myosin distributions in motile and stationary cells. (*A* and *B*) Traction stress maps (*A*) and actin flow maps (*B*) for motile (*Top*) and stationary (*Bottom*) keratocytes. Arrows indicate the direction and magnitude of the traction forces (*A*) and actin network movement with respect the underlying substrate (*B*); hot colors indicate faster flow. (*C–E*) Images of motile (*Top*) and stationary (*Bottom*) keratocytes immunolabeled for the adhesion protein vinculin (*C*, total internal reflection fluorescence images) or myosin (*D*, epifluorescence images) or labeled for actin with fluorescent phalloidin (*E*, epifluorescence images). (*F–I*) Average traction force (*F*), actin flow (*G*), vinculin (*H*), and myosin (*I*) distributions in motile (black line) and stationary (red line) cells are plotted versus cell boundary position. Fluorescent intensities were normalized for each cell by subtracting the mean intensity and dividing by the SD. Error bars are SEM. The images of motile cells in *A–E* are oriented with the leading edge pointed toward the top of the page.

previously described (5, 28), that whereas stationary keratocytes were characterized by slow, centripetal flow of the actin network (average flow rate = 37 ± 4 nm/s, $n = 3$ cells), motile keratocytes were characterized by rapid inward flow of the actin network in the cell rear (267 ± 43 nm/s, $n = 3$ cells) and slow retrograde flow at the leading edge (65 ± 3 nm/s). In both stationary and motile cells, myosin was enriched in regions of the cell that exhibit the most retrograde flow (Fig. 1 *D* and *I*)—to a ring around the cell body in stationary cells and to either side of the cell body in the cell rear in motile cells—consistent with the well-established idea that there is positive feedback between local myosin concentration or activity and actin network flow (5, 23, 28).

These results also suggest a second form of nonlinear feedback—in addition to positive feedback between myosin activity and actin network flow—that could contribute to symmetry breaking in keratocytes. Specifically, we observe that the relationship between actin network flow and traction force generation is different in stationary and motile cells (Fig. 1 *A*, *B*, *F*, and *G*). Stationary cells generate large traction forces and exhibit slow actin network flow, whereas motile cells generate relatively small traction forces despite much faster flow rates. This indicates that the adhesive coupling between the actin network and the underlying surface is lower in the rear of motile cells than in stationary cells, suggesting that adhesions in the prospective cell rear must weaken or break during symmetry breaking in stationary cells. An actin flow-dependent nonlinear switch in adhesion strength has been previously observed in mammalian epithelial cells, with the adhesive coupling between the substrate and the actin network decreasing at a critical actin flow rate (24). We therefore hypothesize that, in keratocytes, negative feedback between actin flow and adhesions in the prospective cell rear in the form of a nonlinear switch in their coupling, as well as positive feedback between flow and myosin, may drive retraction of the cell rear and motility initiation (Fig. 2 *A* and *B*).

A Nonlinear Switch in Adhesion Strength Is Required for Motility Initiation. To understand how these two distinct feedback loops might contribute to symmetry breaking, we set out to develop a general computational model for the balance between myosin

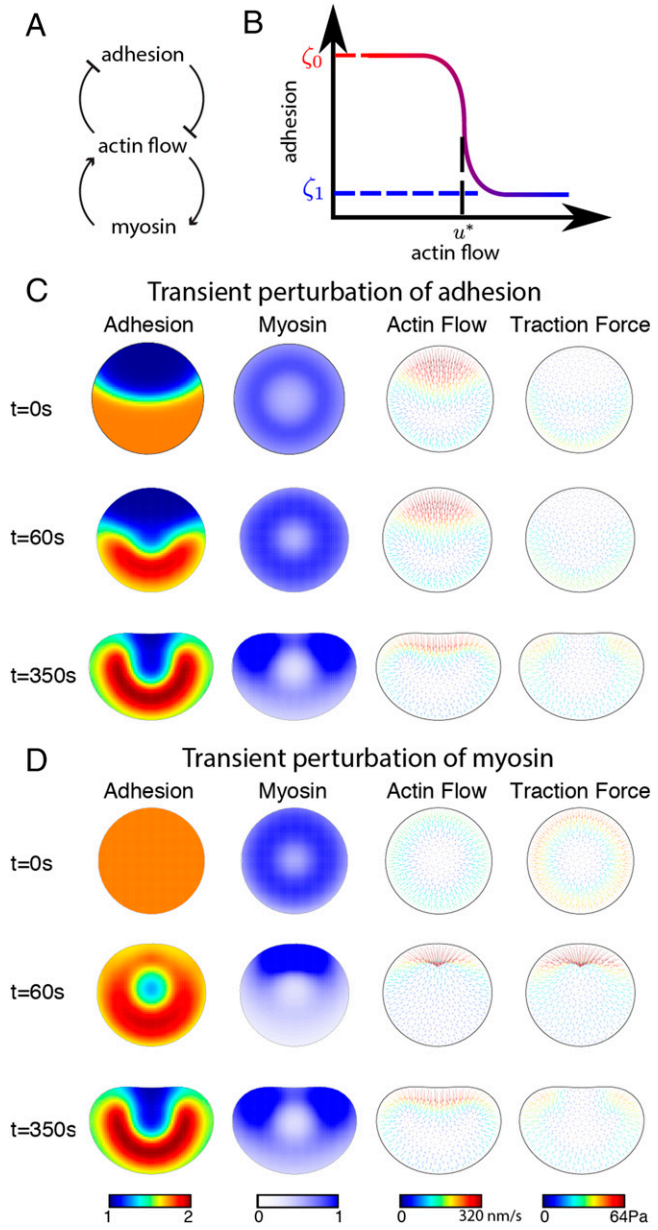

Fig. 2. Simulated traction force, actin flow, adhesion, and myosin distributions in response to transient asymmetries in adhesion strength or myosin density. (*A*) Model simulations incorporate two feedback loops: positive feedback between actin network flow and myosin density and negative feedback between actin flow and adhesion strength. (*B*) Negative feedback between actin flow and adhesion strength is modeled as an actin flow-dependent, nonlinear switch in adhesion strength. Adhesion strength decreases from ζ_0 to ζ_1 when actin flow rates exceed a critical threshold, u^*. (*C* and *D*) Simulated adhesion, myosin, actin flow, and traction force distributions after transient perturbation of adhesion (*C*) or myosin (*D*). The details of the model simulations are described in *SI Text*. In brief, the model simulations were initiated with a circular cell with a fixed boundary and uniform adhesion ($\zeta = \zeta_0$) and myosin densities. The cell boundary was fixed for the first 2 min of the simulation to allow myosin densities and actin flow patterns to equilibrate. Then, the strength of adhesion was reduced (*C*) or the myosin density was increased (*D*) on one side of the cell (t = 0 s). Adhesion, myosin, and actin flow patterns were then allowed to evolve according the rules governing feedback among actin flow, adhesion strength, and myosin density for 1 min. The external adhesion and myosin asymmetries were removed, and the cell boundary was released and allowed to move according to the simulated actin flow patterns (t = 60 s). Transient perturbation of either adhesion strength or myosin density resulted in persistent, rapid movement of fan-shaped cells (t = 350 s).

contraction and adhesion forces applicable to both motile and stationary cells. Our model builds on a recently published model for myosin-driven retrograde flow of the actin network in motile keratocytes (23, 29), described in detail in *SI Text* and Tables S1 and S2. In the context of this model, populations of dynamic adhesion bonds create a frictional slippage interface between the actin network and the underlying surface, generating traction force (21, 22). We assume, therefore, that traction force magnitudes depend on the effective friction coefficient between the cell and the substrate—determined by the number and strength of adhesion bonds—and the rate of actin network flow, relative to the underlying substrate: $\vec{T} = \zeta \vec{U}$. $\vec{T}$ is the traction force exerted by the cell on the underlying substrate through adhesions, ζ is the effective adhesion friction coefficient, and $\vec{U}$ is the rate of actin network flow. Based on our observations of the difference in coupling between actin network flow and traction force between stationary cells (with slow flow and high traction) and at the rear in motile cells (with rapid flow and weak traction), we postulate an actin flow-dependent, nonlinear switch in adhesion strength, as previously observed in mammalian epithelial cells (24), such that the adhesion drag coefficient ζ decreases dramatically when actin flow rates reach a critical threshold (Fig. 2*B*). Based on our actin flow measurements (Fig. 1 *B* and *G*), realistic values for this critical flow rate range from 100 nm/s (greater than the flow rate in stationary cells and at the front in motile cells) to 200 nm/s (less than the flow rate at the rear in motile cells); for our model, we set the critical flow rate to 150 nm/s.

To couple adhesion and traction to myosin activity, we note that, generally, myosin-generated contractile forces are balanced by traction forces: $k\nabla m = \vec{T}$. In this equation, m is the myosin density, k is a proportionality coefficient describing the amount of force produced per myosin unit, and $k\nabla m$ is the gradient of the isotropic myosin-generated stress proportional to the myosin density. In our full model, myosin contraction is also balanced by passive viscous resistance from actin network deformations (see *SI Text*).

In this model, the spatiotemporal distribution of contractile forces, actin network flow, and traction forces depends on the spatiotemporal regulation of the myosin density (m), the amount of force produced by myosin (k), the adhesion friction coefficient (ζ), and the actin network viscosity (η; see *SI Text*). For simplicity, we assume that k and η are constant in space and time, although these are not necessary assumptions. To model the myosin density distribution, we assume, based on previous work (23, 29), that myosin minifilaments bind and move with the actin network (*SI Text*), resulting in positive feedback between myosin localization and actin network flow: As myosin molecules accumulate on the actin network, increased myosin contraction results in increased actin flow and the delivery of additional actin-bound myosin minifilaments.

To determine whether this model, which incorporates negative feedback between actin network flow and adhesion strength in the form of a nonlinear switch, can account for symmetry breaking and motility initiation in response to local up-regulation of myosin activity or local inhibition of adhesion strength, we performed free-boundary model simulations. In these simulations, the cell boundary evolves over time in response to the balance of actin polymerization and inward flow rates. Specifically, the cell boundary remains stationary when actin polymerization and flow rates are equal, protrudes when polymerization is greater than inward flow, and retracts when flow is greater than polymerization (*SI Text*). For simplicity, actin polymerization is maintained at a constant rate in our stimulations (although this is not a necessary assumption), whereas actin flow rates increase with increasing myosin activity and decreasing adhesion strength, in accordance with the model described above. We simulated the effects of either a transient reduction of the adhesion drag coefficient ζ on one side of a stationary cell (Fig. 2*C*) or a transient increase in the myosin concentration (Fig. 2*D*). In these simulations, reduced

adhesion strength and increased myosin activity both resulted in increased actin flow in the cell rear, followed by symmetry breaking and the initiation of persistent motility. Reduced adhesion resulted in immediate and persistent reduction of traction forces in the cell rear, whereas increased myosin caused traction forces in the prospective cell rear to briefly increase before decreasing. Additional model simulations that did not incorporate the actin flow-dependent nonlinear switch in adhesion strength failed to produce realistic symmetry breaking (Figs. S1 and S2; see *SI Text*), suggesting that negative feedback between adhesion and actin flow is required for motility initiation.

A Reduction in Adhesion Strength Immediately Precedes Spontaneous Symmetry Breaking. Our model simulations thus far suggest that transient asymmetries in either myosin density or adhesion strength can trigger symmetry breaking. These predictions, however, are based on simulations in which relatively large and long-lasting asymmetries in adhesion and myosin density are added as external triggers to the model. To determine whether stochastic local fluctuations in either adhesion strength or myosin activity could be amplified by the feedback loops intrinsic to our model to trigger whole-cell symmetry breaking, we added fluctuations to our free-boundary simulations (*SI Text*). In brief, we added spatial–temporal fluctuations of the actin flow to the equations that describe the dynamics of the adhesion drag coefficient, the myosin density, or both. We found that stochastic fluctuations in actin flow rates can trigger spontaneous symmetry breaking and persistent motility (Fig. 3*A* and Fig. S3). The simulated distributions of traction force, actin flow, and myosin density following symmetry breaking were consistent with experimental measurements of these distributions in motile cells (compare Fig. S4 *A–C* and Fig. 1 *F*, *G*, and *I*). A switch in the relationship between traction force and actin flow in the cell rear compared with the cell sides and front was likewise consistent with experimental measurements: Traction forces increased with increasing actin flow rates from the center of the leading edge around the cell perimeter to the sides of the rear but decreased in the center of the rear where flow rates are highest (Fig. S5).

In our simulations, symmetry breaking occurred when local fluctuations persisted for a few tens of seconds and were correlated in space over a few microns (*SI Text*), and model cells that exhibited more variability in traction forces were more likely to break symmetry (Fig. S6). We also found that while the precise time course for the evolution of traction forces during symmetry breaking was variable—either increasing or decreasing in the 5 min before motility initiation, depending on the source of the stochastic fluctuations (see *SI Text*)—in all cases, traction forces and adhesion strength significantly increased and actin flow significantly decreased in the minute before motility initiation (Fig. 3*B* and Fig. S4 *D* and *E*).

These model simulations generated two testable predictions: First, cells that break symmetry should be characterized by more variable traction forces before symmetry breaking compared with cells that remain stationary. Second, traction forces should decrease in the prospective rear immediately before the onset of persistent cell motility. To test these predictions, we measured traction forces generated by nine stationary keratocytes for up to 1 h to determine how traction forces evolve over the course of symmetry breaking (Fig. 3 *C* and *D*). Four of the nine cells initiated motility, and two remained stationary. The remaining three cells exhibited persistent, fluctuating shape changes in the absence of persistent movement; these "shape-shifters" were excluded from subsequent analysis. Cells that remained stationary and those that initiated motility displayed the same average traction force magnitudes, but the SD in forces was significantly higher in cells that initiated motility (Fig. S6 *B–D*), consistent with our first model prediction. Finally, traction forces in the prospective rear decreased in the minute before motility initiation in all four cells, consistent with our second model prediction (Fig. 3*D*, $P = 0.02$, paired t test).

Taken together, the model simulations and traction force measurements described above suggest that an actin flow-dependent reduction in adhesion strength triggers motility initiation. If this is the case, then local inhibition of cell–substrate adhesion should drive symmetry breaking and motility initiation in stationary cells. To test this, we inhibited adhesion on one side of a stationary keratocyte by local application of soluble peptides containing the RGD (Arg-Gly-Asp) integrin-binding motif (30) with a micropipet (Fig. 4 *A* and *C*). Consistent with our prediction, we found that 31% of cells initiated motility, 62% retracted away from the needle, and 7% remained stationary ($n = 13$ cells). Cells that initiated motility continued to move even after the micropipet was removed. Local application of fluorescent dextrans did not induce motility initiation or retraction ($n = 5$ cells). Moreover, we found that local application of soluble RGD peptides to cells that were pretreated with the myosin II inhibitor blebbistatin also induced symmetry breaking and initiated motility (Fig. 4 *B* and *C*): 50% of the cells initiated motility, 33% retracted from the needle, and 17% remained stationary ($n = 6$ cells). Thus, reduced adhesion strength is sufficient for motility initiation even when myosin contraction is inhibited.

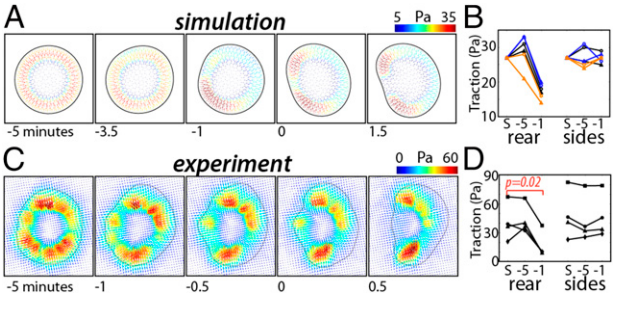

Fig. 3. Traction forces decrease in the prospective rear before motility initiation. (*A* and *C*) Simulated (*A*) and experimental (*C*) traction force maps; arrows indicate direction and magnitude of traction forces. (*B* and *D*) Traction force measurements from six simulations (*B*) and four real cells (*D*). Traction forces in the prospective cell rear and sides are plotted for the start of the simulation or the first imaging frame (S) and 5 min and 1 min before the onset of stable motility (–5 and –1, respectively). For the simulations, stochastic fluctuations were added to actin flow in the dynamic equations for myosin localization (blue lines), adhesion strength (orange lines), or both (black lines).

The Frequency of Motility Initiation Depends on the Balance Between Adhesion and Contractile Forces. In our model, the critical flow rate at which adhesions switch from sticking to slipping ($u^* = 150$ nm/s) represents an instability threshold: Fluctuations that drive the actin flow rate above this threshold trigger negative feedback between actin flow and adhesion strength, eventually causing retraction of the cell rear and motility initiation. We have shown that local inhibition of adhesion triggers motility initiation (Fig. 4); we also predict that global levels of adhesion strength should have an effect on symmetry breaking. Specifically, when adhesion strength is high, the global actin flow rate is low, and vice versa (Fig. S7). As adhesion strength increases, relatively larger fluctuations in actin flow should be required to drive flow rates above the instability threshold, and the frequency of motility initiation should decrease. To test this idea, we plated keratocytes plated on surfaces coated with low, intermediate, or high densities of RGD peptides and measured the fraction of stationary cells that initiated motility after a temperature shift (5). As expected, we found that the frequency of motility initiation increased as adhesion strength decreased (Fig. 5*A*). In addition, since the relative levels of myosin activity and adhesion strength control actin flow rates (23), increasing or decreasing myosin activity should increase or

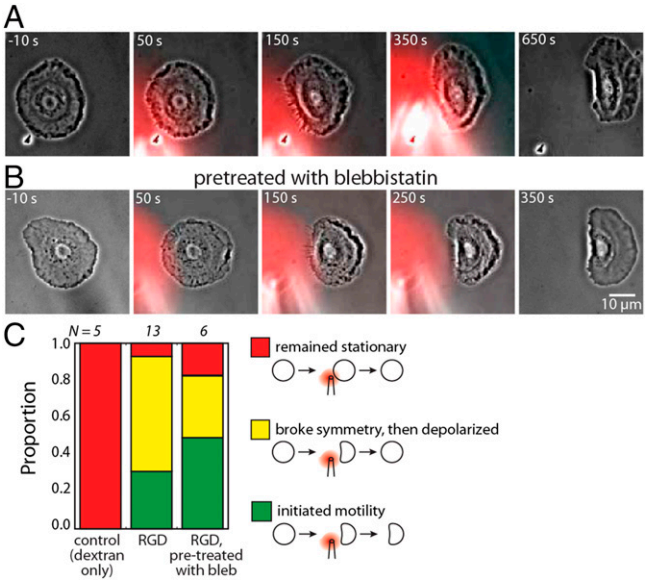

Fig. 4. Local inhibition of cell–substrate adhesion can drive motility initiation. (*A* and *B*) Soluble RGD peptides were applied near stationary cells using a micropipette. The cell in *B* was pretreated with 25 μM blebbistatin for 20 min before RGD application. The cells broke symmetry after RGD application (at $t = 0$ s) and migrated away from the microneedle; both cells maintained polarization and continued to migrate after the RGD peptides were removed (at 500 s in *A* and 275 s in *B*). Red pseudocolor indicates the flow of the RGD peptides away from the pipette. (*C*) The fraction of stationary cells that remained stationary (red), broke symmetry and then lost polarity (yellow), or initiated stable motility (green) after application of Texas Red (TR) dextran alone or TR dextran plus RGD peptides.

decrease the frequency of motility initiation in our temperature shift experiments on all substrates. To test this, we treated cells plated on low, medium, or high RGD densities with either blebbistatin, a myosin II inhibitor (31), or calcyculin A, a phosphatase inhibitor that promotes myosin activity (23, 32). Blebbistatin decreased the fraction of cells that initiated motility on all substrates, whereas calyculin A treatment increased the frequency of motility initiation (d).

Finally, we performed dynamic boundary simulations with stochastic fluctuations around various average myosin and adhesion strengths and, for each parameter set, observed whether the symmetric nonmotile shape remained stable or broke symmetry and initiated motility. These simulations recapitulate our experimental results: When adhesion strength is lowered or myosin is strengthened, the stability of the nonmotile state decreases, resulting in motility initiation (Fig. 5*B*). Altogether, our experimental results and model simulations are consistent with the idea that global adhesion- and myosin-dependent actin flow rates control symmetry breaking by determining how much actin flow fluctuations must be amplified before reaching the critical flow rate at which adhesions switch from gripping to slipping.

Discussion

The initiation of cell migration requires dramatic reorganization of multiple force-generating systems. Here we have presented a mechanical model for symmetry breaking and motility initiation in fish epithelial keratocytes in which stochastic fluctuations in adhesion- and myosin-dependent actin flow are amplified by a nonlinear, flow-dependent switch in adhesion strength. In this model, the critical actin flow rate at which adhesions switch from sticking to slipping sets an instability threshold. Local, stochastic fluctuations in actin flow, myosin localization, or adhesion strength that increase actin network flow above this critical threshold trigger negative feedback between flow and adhesion strength, thereby reducing adhesion strength and further increasing actin flow and myosin accumulation. Amplification of these initial fluctuations eventually results in levels of actin flow high enough to cause retraction of the cell rear and motility initiation.

This model depends on the existence of a nonlinear, flow-dependent switch in adhesion strength. Adhesions are both mechanical structures that transmit forces to the underlying substrate and signaling platforms that localize components of numerous biochemical signaling pathways (21). Rac and Rho GTPase, in particular, have been shown to control adhesion strength and cytoskeletal dynamics (33), and feedback between Rac and Rho signaling networks could, in principle, trigger an actin flow-dependent switch in adhesion strength. However, the critical flow rate for switching adhesions from sticking to slipping in mammalian epithelial cells is impervious to pharmacological perturbation of Rac and Rho GTPase (24), suggesting that signaling is not required for the switch. Instead, a purely mechanical mechanism may be sufficient. Cell–substrate adhesion is mediated by populations of adhesion molecules that link the actin network, through various molecular interactions, to the underlying surface (21). When the actin network moves relative to the underlying surface, these adhesion molecules stretch and detach from the surface with extension-dependent kinetics (34), thereby establishing a frictional slippage interface through which force is exerted on the underlying surface (22). Since adhesion is mediated by a population of adhesion molecules, when actin network flow is slow, a relatively large proportion of adhesion molecules remain bound to the underlying surface at any point in time, and the amount of force transmitted across an individual bond is relatively low. As actin network flow increases, however, fewer and fewer adhesion molecules remain bound to the surface at any point in time, and the amount of force transmitted across an individual bond increases. Eventually, the amount of force transmitted across each individual adhesion bond in the population becomes too great, resulting in detachment of these remaining bonds, and switching the adhesion as a whole from sticking to slipping. Thus, extension-dependent detachment of adhesion molecules, on its own, may be sufficient for an actin-flow-dependent switch in adhesion strength.

Our model for symmetry breaking incorporates two feedback loops: negative feedback between actin flow and adhesion and positive feedback between myosin contraction and actin flow. A recent synthetic biology study (18) suggests that cell polarization

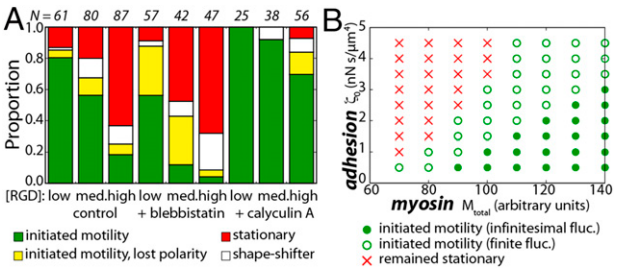

Fig. 5. The balance between myosin contraction and adhesion strength determines the frequency of motility initiation. (*A*) The stability of the symmetric, stationary state was assessed experimentally by measuring the fraction of stationary cells that initiated motility following a temperature shift. (*B*) Numerical simulations of cell boundary dynamics were carried out at the indicated values for ζ_0 (adhesion friction coefficient at low actin flow) and *M* (myosin concentration). At low adhesion or high myosin strength, the symmetric state is unstable (green circles—cells initiate motility instantly in simulations due to very small fluctuations), whereas at high adhesion or low myosin strength, the symmetric state is stable (red crosses). Open green circles indicate the adhesion and myosin strengths at which symmetry breaking requires finite-amplitude fluctuations and takes tens of minutes.

can be achieved by minimal motifs—i.e., positive feedback, or mutual inhibition—under limited conditions, but that circuits combining two or more motifs are significantly more robust. Consistent with this, our results suggest that a single feedback loop may be sufficient for symmetry breaking in stationary keratocytes under extreme conditions. Specifically, positive feedback between actin flow and myosin contraction may be sufficient for symmetry breaking when cell–substrate adhesion strength is low. The rate of actin flow in stationary keratocytes plated on surfaces coated with low densities of adhesion ligands is higher than the critical flow rate at which adhesions switch from sticking to slipping (Fig. S7). This suggests that adhesions in these stationary cells are all slipping, in which case, negative feedback between adhesion and actin flow would not contribute to symmetry breaking. However, these cells break symmetry much more readily than cells plated on surfaces coated with higher densities of adhesion ligands (Fig. 5*A*), suggesting that negative feedback between adhesion and actin flow is not required for symmetry breaking in keratocytes in a low-adhesion state. Our model simulations demonstrate that positive feedback between myosin and actin flow is sufficient for symmetry breaking, with motile cells assuming a nearly round morphology and slow migration speeds following symmetry breaking (Fig. S1), and motile keratocytes plated on surfaces coated with low-adhesion ligand densities are indeed round and slow moving (23). Therefore, it may be that positive feedback between myosin and actin flow is sufficient for symmetry breaking when cell–substrate adhesion strength is low, and that negative feedback between adhesion and flow becomes necessary when adhesion strength increases. Moreover, additional feedback loops, including signaling mechanisms as well as mechanical feedback, may be required for robust motility initiation in other cell types. On the whole, our mechanical model for motility initiation in the relatively simple keratocyte model system provides a framework for understanding symmetry breaking and self-organization phenomena in larger, more complex systems.

Experimental Methods

Keratocyte Culture. Keratocytes were cultured from the scales of the Central American cichlid *Hypsophrys nicaraguensis* as previously described (5).

Traction Force Measurements. RGD-functionalized PAA gels with fluorescent beads embedded near the surface were generated using a modified version of previously published protocols (*SI Text*). Traction forces were measured from cell-induced bead displacements using the Fourier transform traction cytometry method (25).

Actin Speckle Microscopy. The F-actin network in keratocytes was sparsely labeled by electroporation of AlexaFluor546 phalloidin (AF546-phalloidin; Invitrogen), and movement of the actin network relative to the underlying surface was measured using a previously published multiframe correlation algorithm (5, 28) (*SI Text*).

Computational Modeling. The model consists of coupled submodels for viscous flow of the actomyosin network, myosin transport, and adhesion density and strength. We solved the equations of these submodels (described in detail in *SI Text*) using the general public-licensed software FreeFem (available for download at www.freefem.org) designed to solve partial difference equations using finite element methods. The equations were solved on the free-boundary domain as described in *SI Text*.

Additional experimental methods are described in *SI Text*.

ACKNOWLEDGMENTS. We are grateful to Ulrich Schwarz for providing the MatLab code used to analyze traction forces, and to Cyrus Wilson and Gaudenz Danuser for providing the MatLab code used to track actin network flow. This study was supported by National Institutes of Health Grant GM068952 (to A.M.) and by a grant from Howard Hughes Medical Institute (to J.A.T.).

1. Iglesias PA, Devreotes PN (2008) Navigating through models of chemotaxis. *Curr Opin Cell Biol* 20(1):35–40.
2. Zigmond SH, Levitsky HI, Kreel BJ (1981) Cell polarity: An examination of its behavioral expression and its consequences for polymorphonuclear leukocyte chemotaxis. *J Cell Biol* 89(3):585–592.
3. Coates TD, Watts RG, Hartman R, Howard TH (1992) Relationship of F-actin distribution to development of polar shape in human polymorphonuclear neutrophils. *J Cell Biol* 117(4):765–774.
4. Verkhovsky AB, Svitkina TM, Borisy GG (1999) Self-polarization and directional motility of cytoplasm. *Curr Biol* 9(1):11–20.
5. Yam PT, et al. (2007) Actin-myosin network reorganization breaks symmetry at the cell rear to spontaneously initiate polarized cell motility. *J Cell Biol* 178(7):1207–1221.
6. Goehring NW, Grill SW (2013) Cell polarity: Mechanochemical patterning. *Trends Cell Biol* 23(2):72–80.
7. Turing AM (1952) The chemical basis of morphogenesis. *Philos Trans R Soc B* 237(641): 37–72.
8. Loose M, Fischer-Friedrich E, Ries J, Kruse K, Schwille P (2008) Spatial regulators for bacterial cell division self-organize into surface waves in vitro. *Science* 320(5877): 789–792.
9. Wedlich-Soldner R, Altschuler S, Wu L, Li R (2003) Spontaneous cell polarization through actomyosin-based delivery of the Cdc42 GTPase. *Science* 299(5610):1231–1235.
10. van der Gucht J, Sykes C (2009) Physical model of cellular symmetry breaking. *Cold Spring Harb Perspect Biol* 1(1):a001909.
11. Mullins RD (2010) Cytoskeletal mechanisms for breaking cellular symmetry. *Cold Spring Harb Perspect Biol* 2(1):a003392.
12. Howard J (2009) Mechanical signaling in networks of motor and cytoskeletal proteins. *Annu Rev Biophys* 38:217–234.
13. Cameron LA, Footer MJ, van Oudenaarden A, Theriot JA (1999) Motility of ActA protein-coated microspheres driven by actin polymerization. *Proc Natl Acad Sci USA* 96(9):4908–4913.
14. van Oudenaarden A, Theriot JA (1999) Cooperative symmetry-breaking by actin polymerization in a model for cell motility. *Nat Cell Biol* 1(8):493–499.
15. van der Gucht J, Paluch E, Plastino J, Sykes C (2005) Stress release drives symmetry breaking for actin-based movement. *Proc Natl Acad Sci USA* 102(22):7847–7852.
16. Munro E, Nance J, Priess JR (2004) Cortical flows powered by asymmetrical contraction transport PAR proteins to establish and maintain anterior-posterior polarity in the early *C. elegans* embryo. *Dev Cell* 7(3):413–424.
17. Grill SW, Kruse K, Jülicher F (2005) Theory of mitotic spindle oscillations. *Phys Rev Lett* 94(10):108104.
18. Chau AH, Walter JM, Gerardin J, Tang C, Lim WA (2012) Designing synthetic regulatory networks capable of self-organizing cell polarization. *Cell* 151(2):320–332.
19. Cramer LP (2010) Forming the cell rear first: Breaking cell symmetry to trigger directed cell migration. *Nat Cell Biol* 12(7):628–632.
20. Mseka T, Cramer LP (2011) Actin depolymerization-based force retracts the cell rear in polarizing and migrating cells. *Curr Biol* 21(24):2085–2091.
21. Gardel ML, Schneider IC, Aratyn-Schaus Y, Waterman CM (2010) Mechanical integration of actin and adhesion dynamics in cell migration. *Annu Rev Cell Dev Biol* 26:315–333.
22. Chan CE, Odde DJ (2008) Traction dynamics of filopodia on compliant substrates. *Science* 322(5908):1687–1691.
23. Barnhart EL, Lee K-C, Keren K, Mogilner A, Theriot JA (2011) An adhesion-dependent switch between mechanisms that determine motile cell shape. *PLoS Biol* 9(5): e1001059.
24. Gardel ML, et al. (2008) Traction stress in focal adhesions correlates biphasically with actin retrograde flow speed. *J Cell Biol* 183(6):999–1005.
25. Sabass B, Gardel ML, Waterman CM, Schwarz US (2008) High resolution traction force microscopy based on experimental and computational advances. *Biophys J* 94(1): 207–220.
26. Lee J, Leonard M, Oliver T, Ishihara A, Jacobson K (1994) Traction forces generated by locomoting keratocytes. *J Cell Biol* 127(6 Pt 2):1957–1964.
27. Fournier MF, Sauser R, Ambrosi D, Meister J-J, Verkhovsky AB (2010) Force transmission in migrating cells. *J Cell Biol* 188(2):287–297.
28. Wilson CA, et al. (2010) Myosin II contributes to cell-scale actin network treadmilling through network disassembly. *Nature* 465(7296):373–377.
29. Rubinstein B, Fournier MF, Jacobson K, Verkhovsky AB, Mogilner A (2009) Actin-myosin viscoelastic flow in the keratocyte lamellipod. *Biophys J* 97(7):1853–1863.
30. Ruoslahti E, Pierschbacher MD (1987) New perspectives in cell adhesion: RGD and integrins. *Science* 238(4826):491–497.
31. Straight AF, et al. (2003) Dissecting temporal and spatial control of cytokinesis with a myosin II Inhibitor. *Science* 299(5613):1743–1747.
32. Ishihara H, et al. (1989) Calcium-independent activation of contractile apparatus in smooth muscle by calyculin-A. *J Pharmacol Exp Ther* 2:388–396.
33. Guilluy C, Garcia-Mata R, Burridge K (2011) Rho protein crosstalk: Another social network? *Trends Cell Biol* 21(12):718–726.
34. Bell GI (1978) Models for the specific adhesion of cells to cells. *Science* 200(4342): 618–627.